Nigerian Journal of Physics (NJP)
ISSN online: 3027-0936
ISSN print: 1595-0611
DOI: 4https://doi.org/10.62292/njp.v33i4.2024.311
Volume 33(4), December 2024

Fabrication and Characterization of Co and Li Doped TiO_2 Photoanodes for High-Efficiency Dye-Sensitized Solar Cells

[1]Oladosu, O. A., [1,2]Ogundeji, T. S., [3]Adegboyega, O., [4]Ajani, A. S., [4]Egbeyale, G. B., [1]Lana, G. M., [1,5]Awodele, M. K. and *[1,5]Adedokun, O.

[1]Department of Pure and Applied Physics, Ladoke Akintola University of Technology, Ogbomoso, Nigeria.
[2]Department of Basic Science, Adeleke University, Ede, Nigeria.
[3]Department of Physical Science Education, Emmanuel Alayande University of Education, Oyo, Nigeria.
[4]Department of Physics and Materials Science, Kwara State University, Malete, Nigeria.
[5]Nanotechnology Research Group (NANO+), Ladoke Akintola University of Technology, Ogbomoso, Nigeria.

*Corresponding author's email: oadedokun@lautech.edu.ng Phone: +2347031195750

ABSTRACT

The urgent need for a sustainable energy future has driven global efforts to transition from fossil fuels to renewable energy sources. However, challenges such as escalating energy demands, environmental degradation, and the accelerating climate crisis hinder this transition. Dye-sensitized solar cells (DSSCs) emerge as a promising alternative, offering potential advantages like affordability, flexibility, and enhanced efficiency. Titanium (IV) Oxide (TiO_2), a widely studied semiconductor material, has been extensively explored for DSSC applications. However, its inherent limitations, including a wide bandgap, significant charge recombination losses, and low electrical conductivity, impede the development of efficient and cost-effective DSSCs. This study aims to address these challenges and contribute to the advancement of DSSC technology as a viable and sustainable energy solution. DSSCs were fabricated using TiO_2 photoanodes doped with cobalt (Co) and lithium (Li) via a one-pot sol-gel synthesis approach. Ruthenium-based dye N719 was utilized as the sensitizer. Characterization techniques, including XRD, FTIR, DRS, FESEM, and EDX, were employed to analyze the structural, optical, morphological, and elemental properties of the synthesized materials. Doping with Co and Li effectively reduced the TiO_2 bandgap from 3.18 eV to 3.12 eV and 2.88 eV, respectively, leading to enhanced short-circuit current density (Jsc) values of 10.97 mA/cm² and 12.37 mA/cm², respectively. Among the fabricated DSSCs, the Li-doped TiO_2 photoanode demonstrated the highest power conversion efficiency of 5.3%, followed by Co-doped TiO_2 (4.2%) and undoped TiO_2 (3.3%). These findings highlight the potential of Li and Co-doped TiO_2 as promising materials for the development of high-performance DSSCs.

Keywords:
TiO_2,
Co-doped,
Li-doped,
Sol–gel method,
DSSCs,
Performance efficiency.

INTRODUCTION

As energy is a global need for sustainable development on social, economic, and environmental development, it is needed much more often every day for many uses which include livelihoods, water availability, agricultural output, population size, health, and quality education (Galstyan et al., 2022). Fossil fuels, such as coal, oil, and gas, provide the majority of this energy which has been cited among the most influential causes of the global warming(Al Jitan et al., 2020). This continuous increase in the earth's temperature can lead to disastrous effect concerning environment and the earth's climate, which have made humans therefore to look into depending on clean and renewable sources of energy (Omar et al., 2020). The systems from the renewable source of energy are solar systems, wind systems, hydroelectric systems, geothermal systems, biomass systems, hydrogen systems, tidal systems, wave systems and biofuel systems. Of these systems, the solar system which involves the use of the photovoltaic (PV) or Solar Cells, are technology devices that converts sunlight into electricity (Qiu et al., 2021). Several photovoltaic devices that fulfil the energy conversion from sunlight to electricity have already been reported

over the past five decades (Hao et al., 2022). The first photochemical dye-sensitized solar cell (DSSC) was developed by Grätzel and his fellow researchers, and their affordability, simplicity of production, and environmental friendliness attracted a lot of attention (Alamu et al., 2021). DSSC is a promising revolutionary technology for conversion of clean, renewable sunlight into electricity (Andualem & Demiss, 2018). DSSC is a third-generation solar cell that has the potential for future clean energy due to its characteristics of cost effectiveness of fabrication and versatility of fabrication technology (Kokkonen et al., 2021). DSSC comprises of four primary components: a photoanode, a photosensitizer dye, an electrolyte (redox mediator) and counter electrode (Chauke et al., 2024). The photoanode plays a pivotal role in attaining outstanding photo-to-electric conversion efficiency, fulfilling crucial functions such as dye adsorption, electron injection, and electron mobility (Lana et al., 2024). Materials like TiO_2, ZnO and SnO_2 have been used as photoanodes for applications in DSSC (Mohamed, 2019). Among the various materials investigated for their potential in renewable energy applications, TiO_2 has emerged as a promising candidate due to its unique electronic and photovoltaic properties (Aboulouard et al., 2020; Ahmad et al., 2022). TiO_2 is in various phases, with rutile, anatase, and brookite being the most prominent (Chauke et al., 2024). Each phase possesses distinctive properties, including precise energy band gaps, influencing their suitability for diverse applications (Yilleng et al., 2020). Although, TiO_2 can be used as photoanode material in DSSC, its efficiency is comparatively low because of the large bandgap, high recombination losses, and low electrical conductivity (Adedokun et al., 2023). The rutile TiO_2 has a band gap of around 3.0 eV but when well-lighted, electrons in the valence band are excited to the conduction band, generating stable electron-hole pairs with a lower recombination rate compared to anatase (Bahri et al., 2023). Anatase TiO_2, with a wider band gap of about 3.2 eV, experiences similar photoexcitation dynamics. Brookite TiO_2 falls between rutile and anatase in terms of band gap, approximately ranging from 3.2 to 3.4 eV (Hamdan et al., 2020). In the photovoltaic processes of all the TiO_2 phases, the movement of electrons and holes is fundamental. When illuminated with photons carrying energy equal to or greater than the band gap, electrons transition from the valence to the conduction band, creating electron-hole pairs. These charge carriers participate in redox reactions, influencing applications in photovoltaics (El-Kholy et al., 2023). Introducing dopants is found to enhance various qualities of TiO_2, such as the effect of doping on the characteristics of TiO_2 includes structural, morphological, and optical properties and by doping of TiO_2 with suitable dopants like cobalt and lithium, then modified properties can be obtained (Lima et al., 2024). Different methods exist for synthesizing TiO_2 which are sol–gel, spray pyrolysis, solvothermal, microemulsion, precipitation, and electrochemical synthesis methods. Of the presented methods of synthesis, sol-gel is well suitable and convenient for synthesis. It can be considered unique because it does not require high pressures and temperatures of the synthesis and high level of pre-preparation. Thus, sol–gel method is recorded as preferred and often used method of the TiO_2 nanoparticle synthesis because of its advantages such as simplicity, low cost, and versatility (Adedokun et al., 2024). The sol-gel method gives accessibility for synthesizing TiO_2 nanoparticles with different morphologies like sheets, tubes, particles, wires, rods, mesoporous and aerogels (Mushtaq et al., 2020). This method produces high crystal oxides by allowing for control over nanoparticle size, surface morphology, and phase configuration in varying concentration precursors, and it is simple method (Sadek et al., 2022). Sharma *et al* (Sharma et al., 2022) synthesized Co and N doped TiO_2 samples using sol-gel method to increase their photovoltaic characteristics. The photovoltaic investigations revealed a lower band gap of 2.1 eV for the doped TiO_2, as well as better light absorption and charge transport through the formation of localized states. Also, a dip-coating approach was used by Nunea *et al*, (Nunes et al., 2023) to create TiO_2-ZnO composite thin films for photoanodes in DSSCs. The photovoltaic investigations showed that TiO_2-ZnO composite layers increased power conversion efficiency by 1.17%, improved electron transport characteristics, and light absorption. Similarly, a multilayer structure of TiO_2 nanorods and nanotubes was used to improve DSSC photoanode performance by He *et al* (He et al., 2017). The photovoltaic investigations revealed better light absorption, decreased recombination, and increased electron transport, resulting in a higher power conversion efficiency of trilayer NR/NT/NR composite. This work examined the photovoltaic performance of Co and Li doped TiO_2 with the ruthenium dye (N719)-based sensitizer for the fabrication of DSSCs.

MATERIALS AND METHODS

Preparation of Undoped TiO_2

The undoped TiO_2 nanoparticles were synthesized, using sol-gel technique, following the existing procedures by Adedokun *et al* (Adedokun et al., 2023), with titanium isopropoxide (TTIP) as the starting material. 13 ml of 2-Propanol was combined with 10 ml of acetic acid, and after a few mins of stirring, 5 ml of TTIP was added, followed by 15 mins of vigorous stirring. 61 ml of deionized water was then added dropwise and swirled for 1 hr. The solution was allowed to mature for 24 hrs at room temperature before being

dried at 100 °C for at least 2 hrs. The resultant TiO_2 gel was pulverized and then annealed at 500 °C for 3 hrs.

Preparation of Cobalt doped TiO_2

To make cobalt-doped TiO_2, cobalt (II) acetate tetrahydrate mixed in 61 ml of deionized water at room temperature and stir for 30 mins to form a solution X. Solution Y was prepared by dissolving 5 ml of TTIP in 13 ml of 2-propanol and 10ml of acetic acid, which was then agitated for 30 mins. Then solution X was added and carefully dropped into the solution while vigorously swirling. The synthesized doped TiO_2 gel was dried for several hours at 100 °C before being crushed and annealed at 500 °C for three hrs (Adedokun et al., 2024).

Preparation of Lithium doped TiO_2

Similarly, lithium nitrate was mixed in 61 ml of de-ionized water at room temperature and stir for 30 mins to form a solution X. Solution Y was prepared by dissolving 5 ml of TTIP in 13 ml of 2-propanol and 10ml of acetic acid, then stirring for 30 mins. Then, solution X was carefully put into the solution and vigorously stirred for 10 mins. The solution was agitated for 2 hrs at room temperature before being let to mature for 24 hrs. The produced doped TiO_2 gel was dried for many hours at 100 °C. The powder was crushed and annealed at 500 °C for three hrs (Adedokun et al., 2024).

Fabrication of DSSCs

The glass substrates for the photoanode and counter electrode were thoroughly prepared to ensure optimum device performance. The substrates were first ultrasonically cleaned for 30 minutes in a detergent solution, then for another 30 minutes in an acetone and ethanol solution. This facilitated the elimination of contaminants and improved surface adhesion as described by (Alamu et al., 2021). To prepare the sample paste, 0.2 g of sample powder was milled in a porcelain mortar to disaggregate aggregated particles. To reduce particle agglomeration, a solution of 0.5 ml water and 7.5ml ethanol was added progressively throughout the grinding operation. The sample mixture was then homogenized by adding 0.1 g of ethyl cellulose diluted in 1 ml of ethanol. Finally, 1 ml of terpineol was added and well mixed to make a homogeneous mass suited for film production. The counter electrode was made of FTO coated with platinum nanoparticles. The extraction procedures for the natural dyes utilized in the investigation followed established protocols(Adedokun et al., 2020; Alamu et al., 2021). Ruthenizer 535-bisTBA (also known as N719), a ruthenium complex dye, was used as sensitizer. This dye was purchased from Solaronix, SA and prepared in ethanol using 0.5 ml dye solution. Acting on electrolyte being available and solvent volatility, Iodolyte AN-50 Solaronix, SA was chosen as the electrolyte due to its established performance. For device assembly, the prepared photoanode was sensitized by immersing it in the N719 dye solution, then washing with ethanol and air drying. During pasting, a tape spacer was wrapped around the exposed piece of the film electrode, leaving an opening for electrical contact. A drop of liquid electrolyte was added by the capillary technique, and the active surfaces of the photoanode and counter electrode were squeezed together to form a sandwich structure. To achieve perfect sealing and avoid electrolyte evaporation, two binder clips were utilized to secure the electrodes while the sealant cured. The DSSC was then prepared for characterization.

Characterization Techniques

The phase and crystalline structure of TiO_2 were examined using the Rigaku SmartLab X-ray diffractometer at 40 kV and 30 mA. The optical and molecular spectroscopic characteristics of undoped, Co-doped and Li-doped, TiO_2 were studied using the Optics4000 UV-Vis detector light source (HP-2000 BAL Ocean Optics). Diffuse Reflectance Spectroscopy (DRS) experiments were carried out utilizing a coaxial fibre optics cable with an incidence or reflection angle of 45° normal to the sample surface. A Perkin Elmer Fourier Transform Infrared (FTIR) spectrometer was used to evaluate the extracted dye's IR spectra, which revealed information on the chemical structures, functional groups, and bonding. The morphology, particle size, and distribution of the synthesized nanoparticles were investigated using Field Emission Scanning Electron Microscopy (FESEM) with a VEGA TESCAN 3 Model equipped with an energy-dispersive X-ray spectrometer (EDX). The elemental composition, percentage analysis, and purity of the produced metal oxide nanoparticles were assessed by Energy Dispersive X-ray (EDX) analysis using the INCA 200 Model (UK). This systematic and accurate analytical technique allowed for a thorough characterization of the synthesized materials, offering vital insights into their physical, chemical, and optical characteristics.

RESULTS AND DISCUSSION

XRD studies

The structural properties derived from the X-ray diffraction (XRD) patterns on TiO_2, Co-TiO_2 and Li-TiO_2, at room temperature is depicted in Figure 1. Where the diffraction peaks corresponded to planes (101), (112), (004), (200), (105), (211), (204), and (116), with 2θ values of 25.66°, 38.29°, 48.39°, 54.25°, 55.68°, 63.22°, and 69.02° respectively. The anatase phase of TiO_2 exists in all samples, as shown by these peaks. Doping caused a minor shift in the most intense

peak towards higher 2θ values, indicating lattice deformation. The Scherrer equation (Equation 1) was used to calculate the average crystallite size of undoped TiO_2, Co-TiO_2 and Li-TiO_2.

$$D = \frac{0.9\,\lambda}{\beta \cos\theta} \quad (1)$$

where λ is the X-ray wavelength, β is the full width at half maximum, θ is the diffraction angle, and D is the particle diameter size. Table 1 summarizes the calculated crystallite sizes of pure TiO_2 (24.41 nm), Co-TiO_2 (21.15 nm) and Li-TiO_2 (21.19 nm). The observed reduction in crystallite size in Co-TiO_2 shows that Co doping induces lattice strain due to the size difference between Co dopant and Ti ions, resulting to smaller crystallites. This is in agreement with work of Adedokun et al., (Adedokun et al., 2024).On the other side, Li doping resulted in a modest increase in crystallite size, which improve the material's optical transparency and photovoltaic activity. These structural alterations enhance the functional qualities of TiO_2. Adding Co and Li dopants improves TiO_2 samples' light-harvesting, electrical conductivity, and overall performance, making them ideal for photovoltaic and optoelectronic applications.

Table 1: Crystallite size for TiO_2, Co-TiO_2 and Li-TiO_2

Sample	Crystallite size (nm)
Pure TiO_2	24.41
Co- TiO_2	21.15
Li- TiO_2	21.19

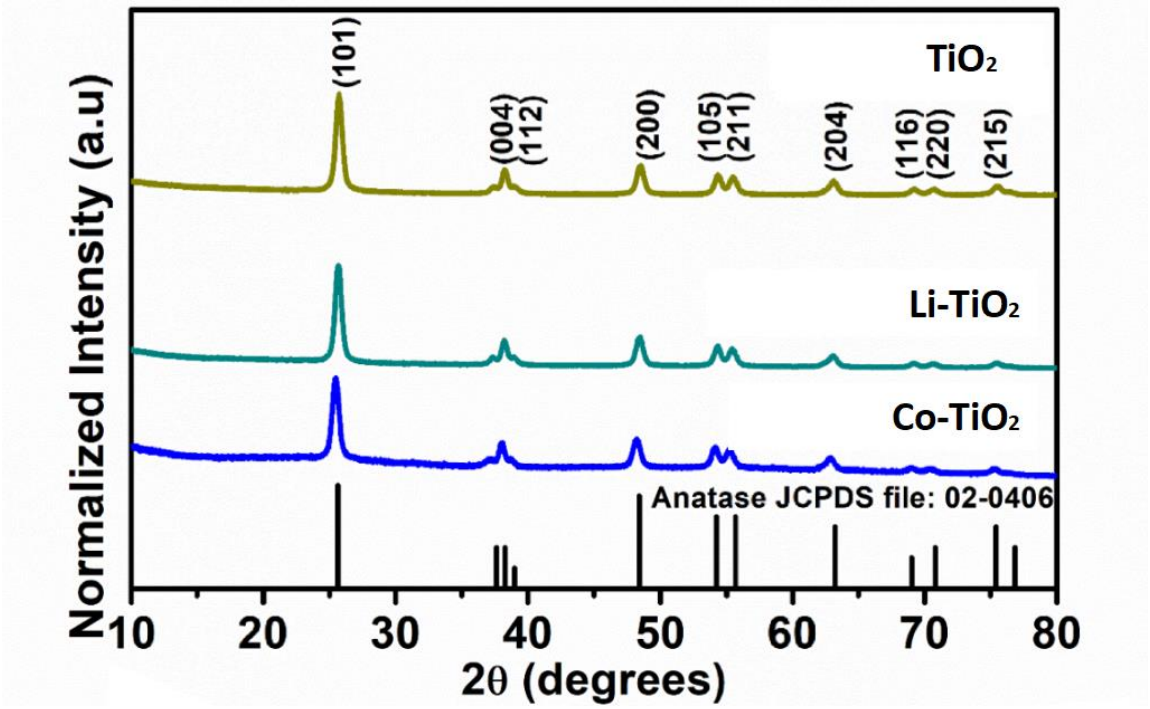

Figure 1: XRD pattern of (a) TiO_2 (b) Li-TiO_2 (c) Co-TiO_2

FTIR spectroscopy

FTIR spectroscopy was used to detect functional groups within the produced samples and are shown in Figure 2. The analysis identified the functional groups present in the samples and their connection to the structural and compositional properties of TiO_2. A wide absorption band between 3200 and 3500 cm^{-1} indicates the stretching vibration mode of the hydroxyl (-OH) bond. This demonstrates the presence of surface hydroxyl groups. The absorption band at 880 cm^{-1} is caused by the bending vibrations of -OH groups in adsorbed water molecules in the synthesized nanoparticles. The low-frequency range (500-900 cm^{-1}) showed a unique absorption band. This band represents the Ti-O-Ti link and demonstrates the effective synthesis of TiO_2. These vibrational properties match the spectra of pure anatase TiO_2. Peaks at 744 cm^{-1} and 500 cm^{-1} indicate TiO_2's anatase polymorph, indicating Ti-O bond stretching. These findings reinforce the structural integrity and phase composition of the synthesized TiO_2, making it suitable for DSSC applications.

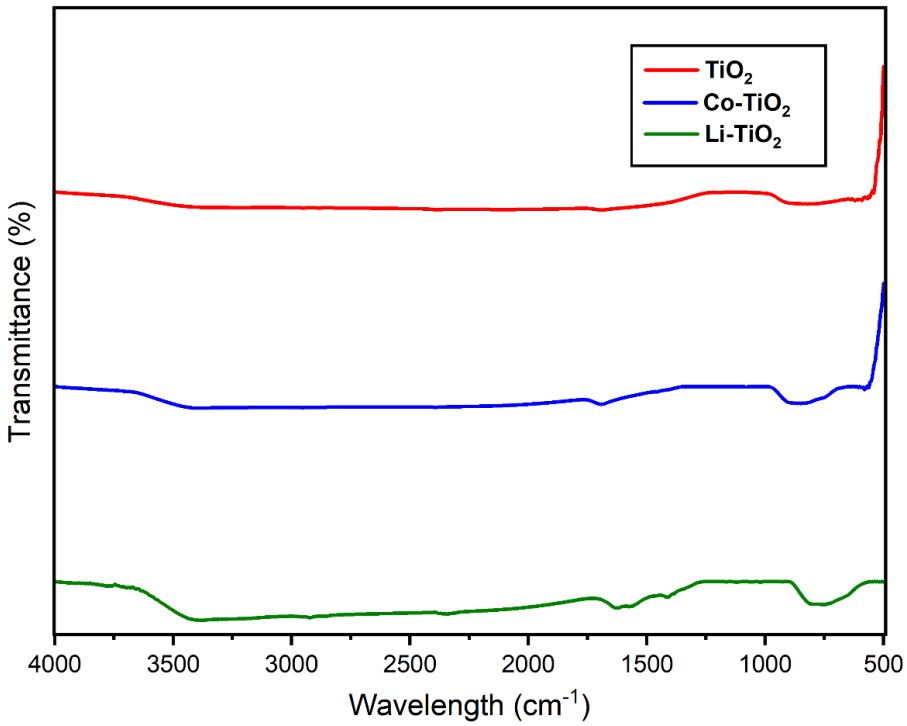

Figure 2: FT-IR spectra for TiO_2, Co-TiO_2, and Li-TiO_2 samples

FESEM-EDX studies

The morphological characteristics of TiO_2, Co-TiO_2, and Li-TiO_2 were examined using FESEM. Figure 3 (A-C) shows micrographs of the produced nanoparticles at magnifications 10µm, revealing deep insights into their structure. The particles have a tetragonal structure and appear as irregularly shaped nanoparticles of various sizes, including big and little jots. The EDX analysis gave qualitative and quantitative data on the elemental composition of the TiO_2, Co-TiO_2, and Li-TiO_2 samples. Figure 3 (D-F) shows the EDX spectrum of the produced TiO_2 nanoparticles, while Figure 4 displays the matching mapping pictures. The analysis revealed the presence of oxygen and titanium as the primary elements, confirming TiO_2 as the dominant phase. For TiO_2, the oxygen content was measured at 39.74% (weight) and 66.38% (atomic), while the titanium content was recorded as 60.26% (weight) and 33.62% (atomic). The Co-TiO_2 samples contained 36.08% (weight) and 63.11% (atomic) oxygen, with titanium contributing 59.85% (weight) and 34.96% (atomic). Additionally, cobalt was detected at 4.06% (weight) and 1.93% (atomic), confirming successful doping. Li-TiO_2 demonstrated oxygen content of 66.14%, with titanium contributing 33.86%, further affirming the dominant tetragonal lattice structure of TiO_2. The analysis revealed the distribution of Ti, O, with the presence of Co, and Li, upholding the effective doping of the TiO_2. The structural and compositional veracity observed in the FESEM and EDX analyses highlights the suitability of these materials for use as photoanodes in DSSCs, where such properties are important for efficient charge transport and light absorption.

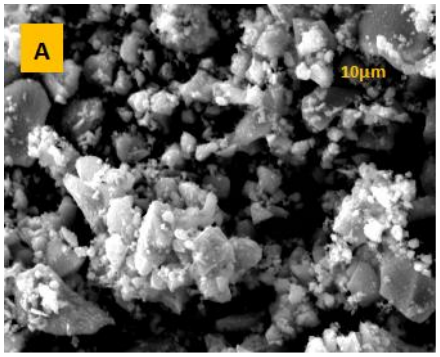

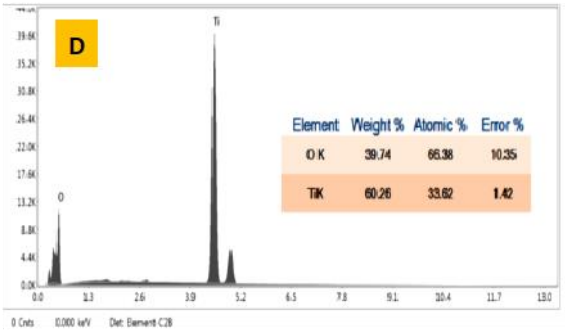

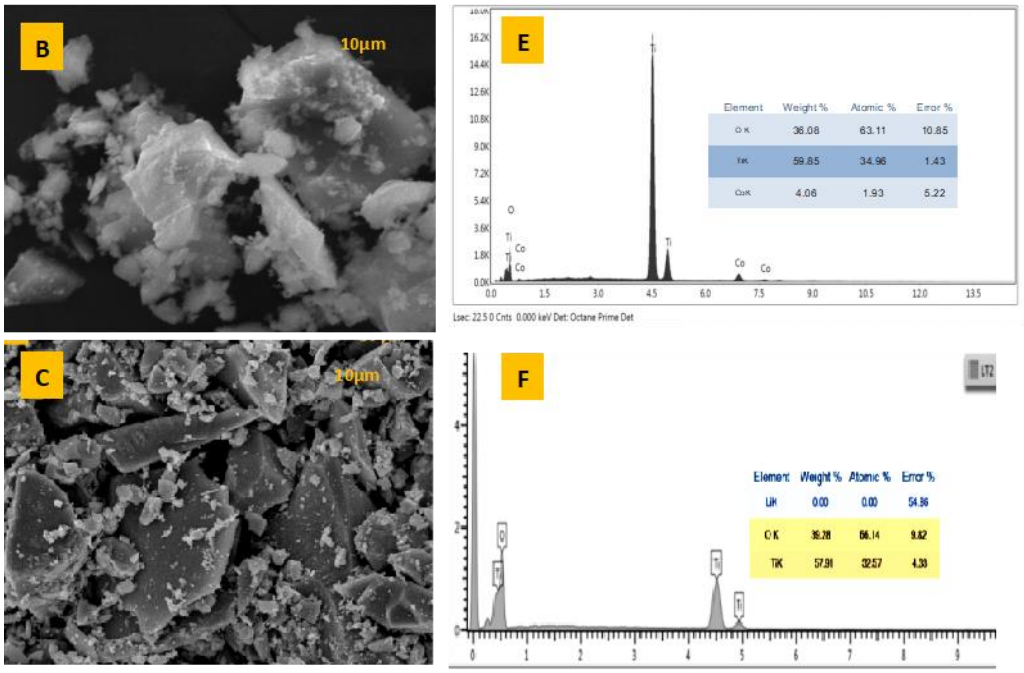

Figure 3: (A–C) SEM micrograph of TiO_2, Co-TiO_2, and Li-TiO_2 (D–F) elemental composition of TiO_2, Co-TiO_2, and Li-TiO_2

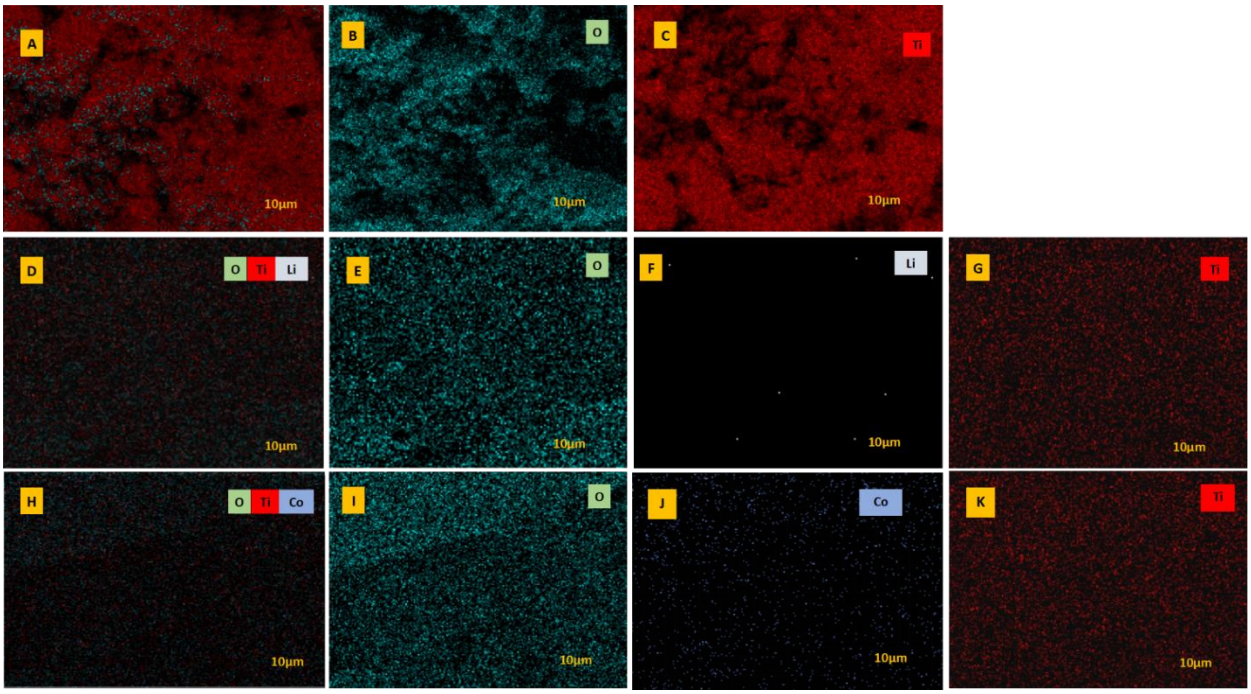

Figure 4: EDX mapping of TiO_2, Co-TiO_2, and Li-TiO_2, and the elemental distribution and mapping of TiO_2 (A–C), Co-TiO_2 (D–G), and Li-TiO_2 (H–K)

Optical Studies

Optical Absorption and Reflectance

The optical absorption and reflectance of TiO_2, Co-TiO_2, and Li-TiO_2 were evaluated using diffuse reflectance scattering (DRS) in the 200-800 nm wavelength range. As shown in Figure 5(A), TiO_2 has a wide absorbance band between 380 and 390 nm, implying restricted photoactivity limited to the UV spectrum. The Co-TiO_2 and Li-TiO_2 bands demonstrated that the addition of dopants causes the absorption band to shift toward wavelengths over 400 nm. Additionally, it was suggested that Co-TiO_2 and Li-

TiO_2 have larger absorption spectra for the visible and ultraviolet light spectrums than TiO_2. The reflectance spectra of TiO_2, Co-TiO_2, and Li-TiO_2 are shown in Figure 5(B), and they shift towards lower wavelengths when each dopant is added. A notable peak is observed at around 400 nm due to the reflectance that occurs during optical transitions. The spectra's measured properties showed a correlation with the work of Adedodun et al. (Adedokun et al., 2024). The energy bandgap was computed with the Kubelka Munk relation from the DRS spectrum.

$$F(R) = \frac{K}{S} = \frac{(1-R)^2}{2R} \quad (2)$$

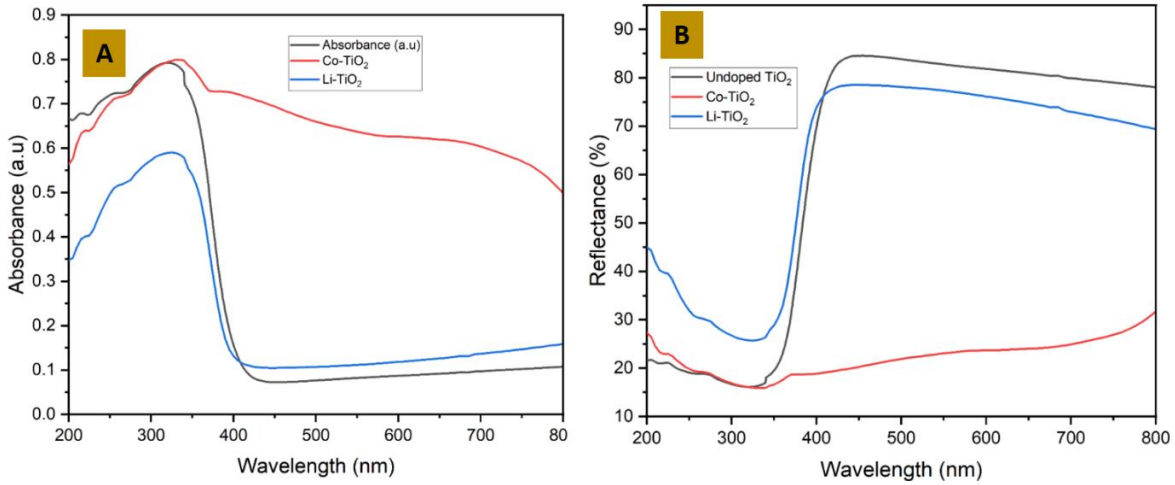

Figure 5: (A) DRS Absorbance plots of TiO_2, Co-TiO_2 and Li-TiO_2. and (B) Reflectance spectra of TiO_2, Co-TiO_2 and Li-TiO_2

Optical Energy bandgap

The optical band gaps for the TiO_2, Co-TiO_2 and Li-TiO_2 are shown in Figure 6. The energy gap decreases as absorbance increases. A decrease in the energy gap implies an increase in the material's conductivity since electrons require less energy to cross through the Fermi level. The energy bandgap was determined using the Tauc plot technique using the Kubelka-Munk formula, where B is constant, hν is the input photon energy, α is the absorbance coefficient, n is constant (n = 2 for direct transition), and E_g is the energy band gap (Alamu et al., 2021). Figure 6 is a graph that explains how the energy bandgap was determined. It also displays the band gap modified TiO_2 nanoparticles, of Co, and Li doped TiO_2 and the undoped TiO_2 (3.18 eV). The bandgap values obtained using this process are summarized in Table 2. The approach gives a reliable estimate of the energy bandgap, which is useful for studying the photovoltaic characteristics of photoanodes in DSSC applications.

The Tauc plot equation, is

$$(\alpha h\upsilon)^n = A(h\upsilon - Eg) \quad (3)$$

In this equation, α is the absorption coefficient, A is constant, and hυ represents photon energy.

And also, Kubelka Munk function was used to modify equation 3 and plot against the photon energy (eV).

Kulbelka Munk equation then given as shown in equation 4 and K is the molar absorption coefficient

$$K = \frac{(1-R)^2}{2R} \quad (4)$$

$$S = 2R \quad (5)$$

S is the scattering factor, R is the reflectance of the material

From our results, we observed decrease in energy band gap with Co and Li doped TiO_2.

As a result, the band-gap energy level of TiO_2 reduced, and the presence of Co and Li dopants caused the absorbance band edge of TiO_2 to fall near to the visible region.

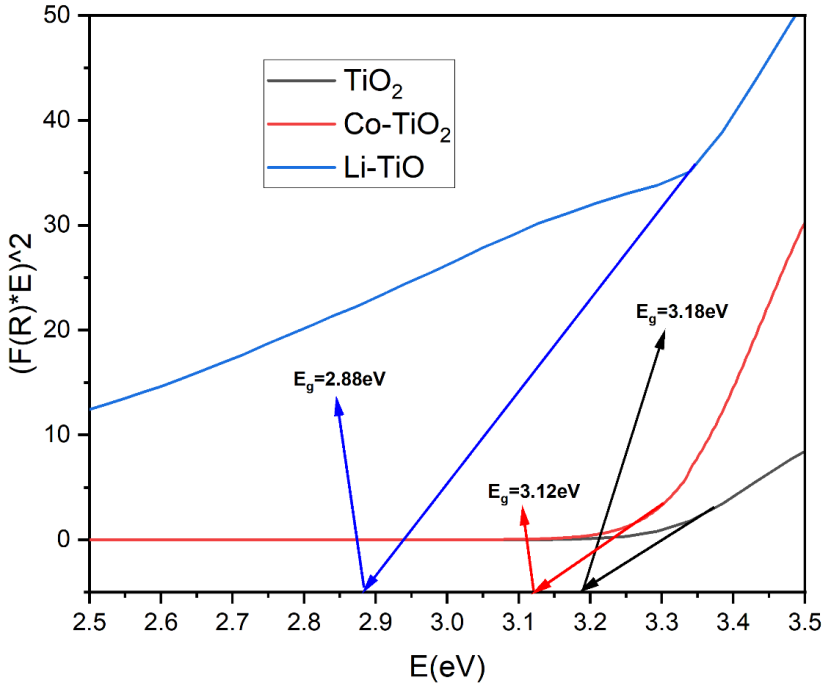

Figure 6: Energy bandgap estimation for TiO_2, Co-TiO_2 and Li-TiO_2

Table 2: Energy bandgap for TiO_2, Co-TiO_2 and Li-TiO_2

Sample	Energy Bandgap (eV)
Pure TiO_2	3.18
Co- TiO_2	3.12
Li- TiO_2	2.88

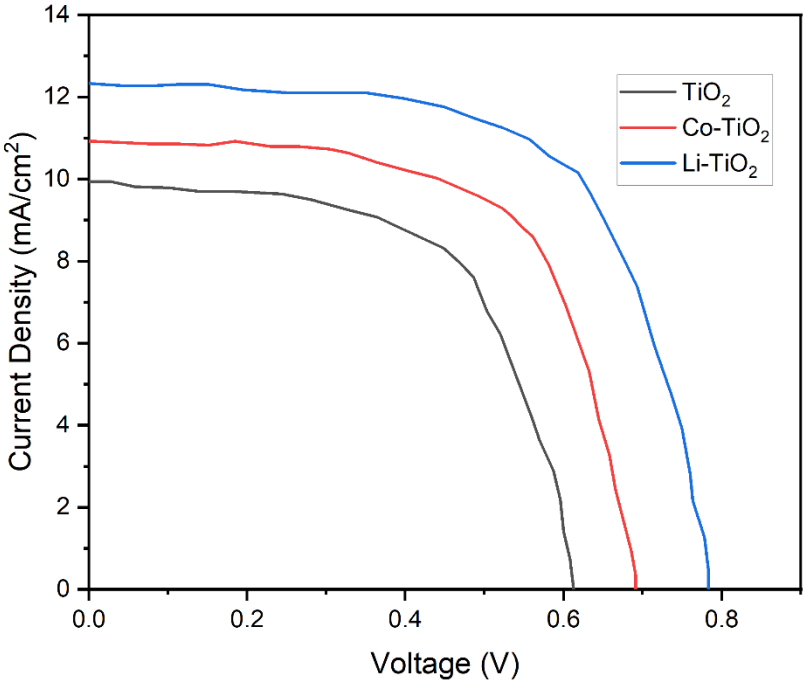

Figure 7: J-V Curves for DSSCs for TiO_2, Co-TiO_2 and Li-TiO_2

Table 3: Photovoltaic parameters of TiO_2, Co-TiO_2 and Li-TiO_2

Sample	Voc (V)	Isc (mA/cm^2)	Fill Factor (FF)	Efficiency (η)
TiO_2	0.61	9.82	0.5511	3.3%
Co- TiO_2	0.69	10.97	0.5674	4.3%
Li- TiO_2	0.78	12.37	0.6021	5.8%

Photovoltaic Performance

DSSCs were characterized to acquire the current density (Jsc) against voltage (V) curves as well as the incident light conversion to electrical measurements. Figure 7 illustrates the current density (J-V) curves of a manufactured DSSC using N719 sensitizer, TiO_2, Co-TiO_2, and Li-TiO_2. The current density rose from 9.82 to 10.97 mA/cm^2 in the presence of Co-TiO_2 and 12.37 mA/cm^2 in the presence of Li-TiO_2. The rise in short current density (Jsc) corresponds to an increase in current due to a greater number of excited electrons moving from the dye's valence band to the conduction band of Co-TiO_2 and Li-TiO_2 (Teixeira et al., 2022). Table 3 shows an overview of the photoelectrochemical characteristics of DSSCs sensitized with ruthenium dye. As shown in Table 3 and Figure 7, the addition of Co and Li increased the efficiency of the TiO_2 nanoparticles. The dopants enhanced the fill factor (FF) and open-circuit voltage (Voc). Voc changes from 0.61 V to 0.69 V for Co-TiO_2 and from 0.61 V to 0.78 V for Li-TiO_2, the short- circuit photocurrent density (J_{SC}) changes from 9.82 mA/cm^2 to 11.1 mA/cm^2 for Co-TiO_2 and from 9.82 mA/cm^2 to 12.37 mA/cm^2 for Li-TiO_2 and its efficiency increased from 3.3% to 4.3% for Co-TiO_2 and from 3.3% to 5.8% for Li-TiO_2 with a 30.3% and 75.76% increase, respectively.

CONCLUSION

In conclusion, this study successfully demonstrated the fabrication of TiO_2, Co-doped TiO_2, and Li-doped TiO_2 nanoparticles via a facile sol-gel method. The synthesized materials were effectively utilized as photoanodes in the construction of DSSCs. The incorporation of Co and Li into the TiO_2 lattice resulted in significant improvements in the optical and morphological properties of the photoanodes. Notably, Li-doped TiO_2 exhibited the most pronounced effects, leading to a substantial reduction in the bandgap and an increase in light absorption. The photovoltaic performance of the DSSCs was significantly enhanced by doping. The Li-doped TiO_2-based DSSC achieved the highest power conversion efficiency of 5.8%, surpassing the undoped TiO_2 device (3.3%) by a considerable margin. The Co-doped TiO_2 device also showed improved efficiency (4.3%) compared to the undoped control. These findings highlight the potential of Co and Li doping as effective strategies for enhancing the performance of TiO_2-based photoanodes in DSSCs. Further optimization of doping concentrations and synthesis conditions may lead to even greater improvements in device efficiency.

ACKNOWLEDGEMENTS

AO gratefully acknowledges the Department of Science & Technology (Govt. of India) for the award of the Research Training Fellowship for Developing Countries Scientists (RTF-DCS).

REFERENCES

Aboulouard, A., Gultekin, B., Can, M., Erol, M., Jouaiti, A., Elhadadi, B., Zafer, C., & Demic, S. (2020). Dye sensitized solar cells based on titanium dioxide nanoparticles synthesized by flame spray pyrolysis and hydrothermal sol-gel methods: A comparative study on photovoltaic performances. *Journal of Materials Research and Technology*, *9*(2), 1569–1577. https://doi.org/10.1016/j.jmrt.2019.11.083

Adedokun, O., Adedokun, O. M., Bello, I. T., Ajani, A. S., Jubu, P. R., Awodele, M. K., Dhlamini, M. S., Kaliamurthy, A. K., & Bhat, M. A. (2024). Sol-gel synthesized lithium-cobalt co-doped titanium (IV) oxide nanocomposite as an efficient photocatalyst for environmental remediation. *Zeitschrift Fur Physikalische Chemie*. https://doi.org/10.1515/zpch-2024-0835

Adedokun, O., Bello, I. T., Sanusi, Y. K., & Awodugba, A. O. (2020). Effect of precipitating agents on the performance of ZnO nanoparticles based photo-anodes in dye-sensitized solar cells. *Surfaces and Interfaces*, *21*(June), 100656. https://doi.org/10.1016/j.surfin.2020.100656

Adedokun, O., Sivaprakash, P., Ajani, A. S., Bello, I. T., & Arumugam, S. (2023). Structural, optical and magnetic studies of sol-gel synthesized Mg-doped pure anatase TiO2 nanoparticles for spintronic and optoelectronics applications. *Physica B: Condensed Matter*, *667*. https://doi.org/10.1016/j.physb.2023.415199

Ahmad, I., Jafer, R., Abbas, S. M., Ahmad, N., Ata-ur-Rehman, Iqbal, J., Bashir, S., Melaibari, A. A., & Khan, M. H. (2022). Improving energy harvesting efficiency of dye sensitized solar cell by using cobalt-rGO co-doped TiO2 photoanode. *Journal of Alloys and Compounds*, *891*, 162040. https://doi.org/10.1016/j.jallcom.2021.162040

Al Jitan, S., Palmisano, G., & Garlisi, C. (2020). Synthesis and surface modification of TiO2-based photocatalysts for the conversion of CO2. *Catalysts*, *10*(2). https://doi.org/10.3390/catal10020227

Alamu, G. A., Adedokun, O., Bello, I. T., & Sanusi, Y. K. (2021). Plasmonic enhancement of visible light absorption in Ag-TiO2 based dye-sensitized solar cells. *Chemical Physics Impact*, *3*, 100037. https://doi.org/10.1016/j.chphi.2021.100037

Andualem, A., & Demiss, S. (2018). Review on Dye-Sensitized Solar Cells (DSSCs). *Journal of Heterocyclics*, *1*(1), 29–34. https://doi.org/10.33805/2639-6734.103

Bahri, S. S., Harun, Z., Wan Salleh, W. N., Hussin, R., Hairom, N. H. H., Kamaruddin, N. H., Basri, H., Rasli, N. I., Rosman, A., Jamaluddin, M. R., & Ainuddin, A. R. (2023). Green Synthesis and Characterization of Fe Doped Tio2 Nanoparticles Using Lawsonia Inermis Leaf Aqueous Extracts As Reductant for Photocatalytic Activity. *ASEAN Engineering Journal*, *13*(3), 141–152. https://doi.org/10.11113/aej.V13.19690

Chauke, N. M., Mohlala, R. L., Ngqoloda, S., & Raphulu, M. C. (2024). Harnessing visible light: enhancing TiO2 photocatalysis with photosensitizers for sustainable and efficient environmental solutions. *Frontiers in Chemical Engineering*, *6*(February), 1–25. https://doi.org/10.3389/fceng.2024.1356021

El-Kholy, R. A., Isawi, H., Zaghlool, E., Soliman, E. A., Khalil, M. M. H., Said, M. M., & El-Aassar, A. elhameed M. (2023). Preparation and characterization of rare earth element nanoparticles for enhanced photocatalytic degradation. *Environmental Science and Pollution Research*, *30*(26), 69514–69532. https://doi.org/10.1007/s11356-023-27090-2

Galstyan, V., Macak, J. M., & Djenizian, T. (2022). Anodic TiO2 nanotubes: A promising material for energy conversion and storage. *Applied Materials Today*, *29*(July). https://doi.org/10.1016/j.apmt.2022.101613

Hamdan, S. A., Ibrahim, I. M., & Ali, I. M. (2020). Comparison of anatase and rutile TiO2 nanostructure for gas sensing application. *Digest Journal of Nanomaterials and Biostructures*, *15*(4), 1001–1008. https://doi.org/10.15251/djnb.2020.154.1001

Hao, D., Qi, L., Tairab, A. M., Ahmed, A., Azam, A., Luo, D., Pan, Y., Zhang, Z., & Yan, J. (2022). Solar energy harvesting technologies for PV self-powered applications: A comprehensive review. *Renewable Energy*, *188*, 678–697. https://doi.org/10.1016/j.renene.2022.02.066

He, Z., Li, J., Wang, D., Wang, J., & Zhang, T. (2017). Enhanced photovoltaic performance of TiO2 dye-sensitized solar cell based on one-dimensional composite photoanode. *International Journal of Electrochemical Science*, *12*(10), 8918–8928. https://doi.org/10.20964/2017.10.02

Kokkonen, M., Talebi, P., Zhou, J., Asgari, S., Soomro, S. A., Elsehrawy, F., Halme, J., Ahmad, S., Hagfeldt, A., & Hashmi, S. G. (2021). Advanced research trends in dye-sensitized solar cells. *Journal of Materials Chemistry A*, *9*(17), 10527–10545. https://doi.org/10.1039/d1ta00690h

Lana, G. M., Bello, I. T., Adedokun, O. M., Adenigba, V. O., Jubu, P. R., Adedokun, O., Sanusi, Y. K., Dhlamini, M. S., & Awodugba, A. O. (2024). One-Dimensional TiO2 Nanocomposite-based Photoanode for Dye-Sensitized solar Cells: A review. In *Solar Energy* (Vol. 279). Elsevier Ltd. https://doi.org/10.1016/j.solener.2024.112850

Lima, F. M., Leitão, J. S. O., Nunes, V. F., Andrade, M. R., Santana Mota, J. P., de Moura, T. A., Leite Almeida, A. F., de Amorim, A. F. V., Girão, D. de C., Aguiar Freire, F. N., & Rocha, J. S. (2024). Tin Dioxide-Based Photoanodes Integrated Into the Dye Sensitized Solar Cells Structure. *Materials Research*, *27*, 1–10. https://doi.org/10.1590/1980-5373-MR-2024-0042

Mohamed, D. (2019). Preparation and characterization of Titanium dioxide and Zinc oxide thin films via Sol-Gel (spin coating) technique for optoelectronic applications Speciality: Physics of thin films.

Mushtaq, K., Saeed, M., Gul, W., Munir, M., Firdous, A., Yousaf, T., Khan, K. B., Sarwar, H. M. R., Riaz, M. A., & Zahid, S. (2020). Synthesis and characterization of TiO2 via sol-gel method for efficient photocatalytic degradation of antibiotic ofloxacin. *Inorganic and Nano-Metal Chemistry*, *50*(7), 580–586. https://doi.org/10.1080/24701556.2020.1722695

Nunes, V. F., Lima, F. M., Teixeira, E. S., Maia, P. H. F., Almeida, A. F. L., & Freire, F. N. A. (2023). Synthesis of TiO2/ZnO photoanodes on FTO conductive glass for photovoltaic applications. *Ceramica*, *69*(389), 79–86. https://doi.org/10.1590/0366-69132023693893383

Omar, A., Ali, M. S., & Abd Rahim, N. (2020). Electron transport properties analysis of titanium dioxide dye-

sensitized solar cells (TiO2-DSSCs) based natural dyes using electrochemical impedance spectroscopy concept: A review. *Solar Energy*, *207*(September), 1088–1121. https://doi.org/10.1016/j.solener.2020.07.028

Qiu, Y., Zhang, P., Li, Q., Zhang, Y., & Li, W. (2021). A perfect selective metamaterial absorber for high-temperature solar energy harvesting. *Solar Energy*, *230*, 1165–1174. https://doi.org/10.1016/j.solener.2021.11.034

Sadek, O., Touhtouh, S., Rkhis, M., Anoua, R., El Jouad, M., Belhora, F., & Hajjaji, A. (2022). Synthesis by sol-gel method and characterization of nano-TiO2 powders. *Materials Today: Proceedings*, *66*, 456–458. https://doi.org/10.1016/j.matpr.2022.06.385

Sharma, A., Negi, P., Konwar, R. J., Kumar, H., Verma, Y., Shailja, Sati, P. C., Rajyaguru, B., Dadhich, H., Shah, N. A., & Solanki, P. S. (2022). Tailoring of structural, optical and electrical properties of anatase TiO2 via doping of cobalt and nitrogen ions. *Journal of Materials Science and Technology*, *111*(December), 287–297. https://doi.org/10.1016/j.jmst.2021.09.014

Teixeira, E. S., Nunes, V. F., Pinho, D. C., Maia, P. H. F., Lima, F. M., de Sá Moreira, M., Almeida, A. F. L., & Freire, F. N. A. (2022). Effect of the Performance of Lignin Into the Matrix of the TiO2 with Application on DSSCs. *Floresta e Ambiente*, *29*(3). https://doi.org/10.1590/2179-8087-FLORAM-2022-0013

Yilleng, M. T., Sunday, M., & Stephen, D. (2020). Synthesis, Characterization and Photoactivity Evaluation of Nitrogen Doped Titanium Dioxide on Methylene Blue Dye Degradation. *Fudma Journal of Sciences*, *4*(3), 148–153. https://doi.org/10.33003/fjs-2020-0403-356